Hydrogen Bonding versus Ion Pairing in Polyelectrolyte Multilayers with Homopolynucleotides

Marie Z. Markarian, Maroun D. Moussallem, Houssam W. Jomaa, and Joseph B. Schlenoff*

Department of Chemistry and Biochemistry, Center for Materials Research and Technology (MARTECH), The Florida State University, Tallahassee, Florida 32306

Received May 18, 2006; Revised Manuscript Received August 21, 2006

Homopolynucleotides—poly(adenylic acid), poly(A), and poly(uridylic acid), poly(U)—were assembled, layer-by-layer, into thin films with poly(ethylenimine), PEI. Various combinations and sequences of polynucleotide and PEI were used to highlight contributions of electrostatic versus hydrogen bonding as driving forces for multilayer build-up. Assembly of alternating poly(A) and poly(U) failed to yield growing films, due to excessively strong interactions between these complimentary strands. The surface morphology of multilayers depended on the deposition order and whether films had been annealed by salt. Films assembled from preformed A/U duplexes (having high persistence lengths) were very smooth. Individual adsorption steps, followed by optical waveguide light-mode spectroscopy, showed that only complementary polynucleotides adsorb by H-bonding to the surface of a growing multilayer. In contrast to behavior usually observed for polyelectrolyte multilayer build-up, the films decreased in thickness with increasing salt concentration.

Introduction

Interest in polynucleotides for technological and medical applications is currently very strong. DNA has been used for synthesis of patterned surfaces by immobilization of nucleotide strands onto cationic lipid bilayers.[1] Both metallic and insulating substrates have been prepared,[2] and recently, fabrication of nucleotide microarrays was achieved.[3] DNA-containing assemblies are being employed as biosensors[4−6] and in electronics.[7] In addition to the latter applications, polynucleotides are being explored for drug delivery[8] as well as gene delivery and therapy.[9−11]

To date, most assemblies have been formed by deposition of a polynucleotide monolayer onto a modified surface.[12,13] Three-dimensional architectures have been produced by incorporation of polynucleotides into polyelectrolyte structures,[9,14,15] mainly in multilayers built via the layer-by-layer (LbL) assembly protocol.[16−18] Applications of the LbL protocol have been growing since its debut due to the simplicity of the method: substrates are alternately introduced into positively and negatively charged polyelectrolyte solutions, yielding a thin coating on the surface of the substrate.

The build-up mechanism consists mainly of ion-pairing, or "electrostatic," interactions between the oppositely charged polyelectrolytes, summarized in the following equation, which represents the adsorption of a polyanion onto a positively charged polycation surface:

$$\mathrm{Pol^+Cl^-_{(surface)}} + \mathrm{Pol^-Na^+_{(aq)}} \rightarrow \mathrm{Pol^+Pol^-_{(surface)}} + \mathrm{Na^+_{(aq)}} + \mathrm{Cl^-_{(aq)}} \quad (1)$$

Such electrostatic interactions have been thoroughly studied.[19−23] Other interactions, such as hydrophobic interactions, van der Waals, and hydrogen bonding, have also been investigated.[24−26] Hydrogen bonding within polyelectrolytes[27−33] has been used to assemble multilayers from poly(*N*-isopropylacrylamide) and poly(styrene sulfonate-*co*-maleic acid)[30] and from poly(*N*-vinylpyrrolidone) and poly(methacrylic acid).[29]

Attempts have also been made to build multilayers from similarly charged polyelectrolytes. Lowack and Helm[35] and Fischer and Laschewsky[34] showed the limited growth of multilayers from positively charged polyelectrolytes. Recently, Johnston et al.[36] assembled negatively charged DNA oligonucleotides into multilayers through specific hydrogen bonding. We were interested in forming multilayers using polyelectrolytes capable of hydrogen and/or electrostatic interactions. The effect of ionic concentration (salt) was considered an important variable, as salt is an important factor controlling the growth of the thin films, inducing interpenetration and diffusion of polyelectrolytes within multilayers.[19,37−41] Like-charged hydrogen bonding systems such as polynucleotides interact more strongly in the presence of salt, whereas oppositely charged polyelectrolytes are more weakly bound as salt concentration increases.

Experimental Section

Poly(ethylenimine), PEI (50 wt % solution in water, molecular mass ∼750 kDa); poly(adenylic acid) potassium salt, poly(A) (molecular mass ∼200−700 kDa by low angle laser light scattering, LALLS); poly(cytidylic acid) potassium salt, poly(C) (molecular mass ∼118 kDa by LALLS); and poly(uridylic acid) potassium salt, poly(U) (molecular mass >800 kDa by electrophoresis) were used as received from Aldrich. Sodium phosphate monobasic, NaH_2PO_4; sodium phosphate, Na_2HPO_4; sodium chloride, NaCl; and sodium hydroxide, NaOH (1 N solution) were obtained from Fisher Scientific. All chemicals were used without further purification.

Multilayers were prepared, either manually or with the aid of a robot, on Si⟨100⟩ (Topsil Inc.) and quartz substrates (G.M. Associates, Inc.), cleaned in "piranha" solution [7:3 H_2SO_4 (concentrated) and 30% H_2O_2 (*caution: piranha should not be stored in closed containers*)]. Films for the LbL build-up study were prepared manually. The wafer was alternately dipped in 5 mM PEI (polyelectrolyte concentration based on the repeat unit) and in 0.5 mM polynucleotide solutions for 10 min

10.1021/bm0604909 CCC: $37.00
Published on Web 12/01/2006

Table 1. Summary of the Multilayer Repeat Units Used, Termed Systems I−V

system	polyelectrolyte "repeat unit"	interactions
I	poly(A)/poly(U)	H-bonding
II	PEI/poly(A)/PEI/poly(U)	electrostatic, (H-bonding)
III	PEI/poly(A)/poly(U)	electrostatic, H-bonding
IV	PEI/poly(AU)	electrostatic, H-bonding
V	PEI/poly(U)	electrostatic

each. After each layer, the wafer was rinsed three times, followed by a fourth rinse in water, and finally dried with N_2. Thickness was measured with a Gaertner Scientific L116B autogain ellipsometer, using a 632.8 nm laser at 70°. All solutions, including rinses, were prepared in 0.15 M NaCl in 25 mM phosphate buffer at pH 7.2.

Multilayers for surface morphology and salt effect studies were built by a robot (nanoStrata Inc.). Si or quartz was fixed on the end of a stainless steel spindle with Teflon tape and rotated at 300 rpm by a dc motor. The robot was programmed to alternately expose the substrate to the polymer solutions for 5 min each, followed by three rinses in the NaCl/buffer solution for 30 s. Each multilayer contained a total of 20 or 21 layers of polyelectrolyte. The film was then rinsed in water and dried under N_2.

UV−Visible and circular dichroism spectra were respectively collected with a Varian spectrophotometer (Cary, 3-E) and circular dichroism spectrometer (Jasco J-810). Surface images and roughness measurements were acquired with an atomic force microscope, AFM (Dimension 3001, Nanoscope IV, Digital Instruments, Inc.) in intermittent contact mode, and the thickness of thin films for the salt study was determined by a profiler (KLA-Tencor, P-15). For the latter experiment, the NaCl concentration in the polyelectrolyte solutions and rinses, used for build-up, was varied from 0 to 0.8 M.

The growth of multilayers was also followed, in situ, by optical waveguide lightmode spectroscopy, OWLS. Data were acquired with a Bios-1 goniometer (Artificial Sensing Instruments, Zürich). An optical waveguide grating coupler sensor chip was used as substrate, which is coated with silicon titanium oxide, $Si_xTi_{(1-x)}O_2$ ($x = 0.25 \pm 0.05$), with a refractive index of 1.77 ± 0.03. It had a 20 nm diffraction grating depth and a periodicity of 2400 mm^{-1}. All solutions used were prepared with filtered phosphate-buffered saline solution at pH 7.2 and 0.15 M NaCl (filters from Whatman, Anotop 25, 0.45 μm). A clean sensor chip was inserted in the sample holder and buffer solution was pumped through for 10 min (pumping speed 8.3 $\mu L\ s^{-1}$). The buffer solution was left to stand on the grating system to create a homogeneous environment by filling in the grating lines. Polyelectrolyte multilayers (PEMUs) were built by flowing polyelectrolyte solutions, alternately, for 4 min, followed by rinsing with buffer, also for 4 min. A constant temperature was maintained throughout each experiment.

Results and Discussion

In addition to their pervasive hydrogen bonding interactions, the negatively charged phosphate backbone of the polynucleotide chains enables them to behave as polyelectrolytes. Hence it is possible to assemble them within multilayered polyelectrolyte matrices. We studied the build-up of PEI/RNA multilayers via the layer-by-layer build-up protocol. Poly(A) and poly(U) were the strands of choice as they are complimentary polynucleotides. We have built multilayers via multiple combinations and deposition sequences of PEI and homopolynucleotides, which are represented as systems I−V. The naming and the interactions within the different systems are summarized in Table 1. In Figure 1 we show the layer-by-layer build-up of four different multilayer systems. In system I, poly(A) and poly(U) were alternately deposited on a silicon wafer primed with a single layer of PEI, represented by the nomenclature PEI[poly(A)/poly-(U)]$_x$. System II shows the build-up of alternating bilayers of PEI/poly(A) and PEI/poly(U), represented by [PEI/poly(A)/PEI/poly(U)]$_x$. In system III, the assembly of [PEI/poly(A)/poly-(U)]$_x$ was performed where a layer of poly(A) was built on PEI, followed by the addition of poly(U) on poly(A). In system IV, double-stranded poly(AU) was deposited on PEI, yielding a multilayer that can be noted as [PEI/poly(AU)]$_x$. Finally, system V corresponds to PEI and poly(U) deposited to give the [PEI/poly(U)]$_x$ multilayer.

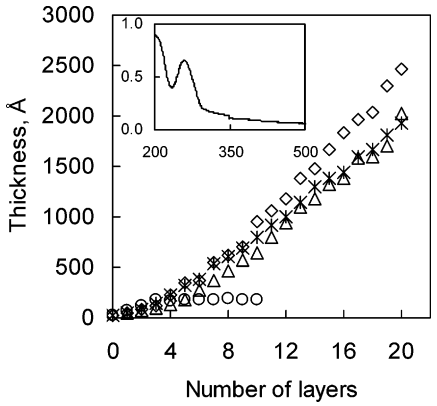

Figure 1. Layer-by-layer build-up of PEI and RNA polyelectrolytes from solutions at 0.15 M NaCl in 25 mM phosphate buffer, pH 7. (○) System I, PEI/[poly(A)/poly(U)]$_{4.5}$; (△) system II, [PEI/poly(A)/PEI/poly-(U)]$_5$; (◇) system III, [PEI/poly(A)/poly(U)]$_7$; (*) system IV, [PEI/poly-(AU)]$_{10}$. (Inset) UV-Visible spectrum of system III deposited on quartz substrate. The peak at 260 nm is characteristic of purine and pyrimidine bases in DNA and RNA.

Layer-by-Layer Build-up. In system I, which eventually relies on H-bonding only, an increase in thickness was observed, but the build-up levels off after the fourth layer and remains constant at a thickness of 173 ± 5 Å. The first step, that is, the addition of poly(A) on the PEI layer, is a result of electrostatic interactions. When the PEI/poly(A)-modified substrate is dipped in poly(U), we observe a further addition of polyelectrolyte on the surface. Previous studies have shown that with interrupted depositions of polyelectrolytes and drying steps within the different layers of the multilayer, deposition of similarly charged polyelectrolyte is possible as a result of interpenetration of the polyelectrolytes.[34,35,42] We believe the further addition of negatively charged polymers onto the bilayer is due to hydrogen bonding between the complementary bases of poly(A) and poly-(U).

Recent work by Johnston et al.[36] demonstrated build-up of negatively charged oligonucleotides via hydrogen bonding. By employing a two-block nucleotide system they were able to mimic the charge overcompensation phenomenon of multilayers. The growth observed was similar to that of the poly(styrene sulfonate), PSS, and poly(allylamine hydrochloride), PAH, polyelectrolyte pair. In addition, they carried out a similar deposition sequence, as in system I, by alternately depositing A_{30} and T_{30} oligomers.

In our study, the limited growth of system I is probably due to a lack of overcompensation of each new layer relative to the previous one, coupled with slow interdiffusion kinetics. In general, weakly interacting systems form thicker multilayers. For example, some hydrophilic polyelectrolytes are able to overcompensate the entire growing multilayer, leading to exponential growth. PAH/PSS is a strongly interacting system that forms thin multilayers.[37] Complementary polynucleotides are designed to interact strongly over long correlation lengths, leading to efficient base pairing with no bases left over (i.e., no overcompensation). Multiple interactions between polynucle-

otides are also expected to prevent interdiffusion, effectively "locking" layers in place.

In an effort to promote regular build-up from RNA, we included a mixture of electrostatic and H-bonding mechanisms. The first permutation is system II. Curvature to the fourth layer is followed by a linear growth of the structure where charge overcompensation has reached a constant value. Initially, we believed minimal specific hydrogen bonding would exist in the assembly as the homopolynucleotides would be separated by a layer of PEI. To provide an intermediate opportunity for H-bonding, we assembled films following the sequence of system III. As in the previous case, slow growth exists up to the fourth layer, after which linear growth of the multilayer is observed. Poly(A) is readily added to the PEI layer via attractive electrostatic interactions. Hydrogen bonding between U and A bases allows the addition of the third layer, which is followed by the electrostatic addition of PEI, etc.

For comparison, a film from PEI and double-stranded poly(AU) polymer, formed separately in buffered saline, was built (system IV). The build-up observed was similar to that of systems II and III. The result implies that whether single- or double-stranded polynucleotides are used to build the multilayer, the charge density brought onto the surface of the PEI layer is of similar order; that is, similar overcompensation effects are observed in the two build-up strategies. The fact that similar build-up is observed for systems II, III, and IV suggests that there is enough interpenetration to enable participation of both electrostatic and H-bonding interactions, even for system II, where the H-bonding is nominally separated by a layer of PEI.

Surface Morphology. While the layer-by-layer study of systems II−IV did not reveal a difference in the build-up, AFM experiments showed surface morphological differences between the multilayers (Figure 2). Panel A depicts the topology of film corresponding to system II. The build-up is thought to be mainly based on electrostatic interactions of the PEI chains with the phosphate backbone of the polynucleotides. Similar to previous AFM studies of polyelectolyte films,[37,43−46] analysis of a 1 × 1 μm^2 surface area of the [PEI/poly(A)/PEI/poly(U)]$_4$ multilayer revealed vermiculite-type morphology with an rms roughness of 12 nm (summarized in Table 2).

Turning to system III (Figure 2B), we see a clear difference compared to system II. The surface of the film appears to be rougher than that of the film in panel A, as bigger blobs are on the surface. Accordingly, 1 × 1 μm^2 areas show an rms roughness of 30 nm. The increase in roughness can be associated with the addition of a third layer of negatively charged poly(U) on the surface, which is thought to be bound to poly(A) by hydrogen bonding. As the polynucleotides are tightly held together through H-bonding, their diffusion becomes limited; therefore, given the time scale of the deposition of poly(U), there can be no or minimal interpenetration of poly(U) to the surface of PEI to create intrinsic electrostatic interactions with the polycation, hence the roughness of the multilayer. For comparison purposes, a [PEI/poly(AU)]$_{10}$ film was prepared on a silicon substrate. Double-stranded polynucleotides are relatively ordered polymer helices with much greater persistence length and therefore rodlike structures. The persistence length, l_p, of single-stranded polynucleotide is 78 Å,[47] whereas l_p of double-stranded polynucleotide is 638 Å.[48] A RNA pair with such a high aspect ratio is expected to adsorb flat to the surface, yielding very smooth surface features. The resulting poly(AU) multilayer exhibited an rms value of 5 nm (Figure 2C).

Surface and roughness studies performed by Dubas and Schlenoff[37] showed that annealing in NaCl decreases the roughness of a polyelectrolyte multilayer. For example, a PSS/PDADMA [poly(diallyldimethylammonium chloride)] becomes much smoother after a few hours' immersion in 0.5 M NaCl. Annealing introduces counterions ("extrinsic compensation") into multilayers, decreasing interactions between polyelectrolytes and allowing them to move faster.[38] In order to investigate the effect of annealing on the polyelectrolyte systems, we immersed the multilayers in 0.5 M NaCl in 25 mM phosphate buffer, pH 7, for 12 h (Table 2). The roughness of the roughest system decreased by 76%.

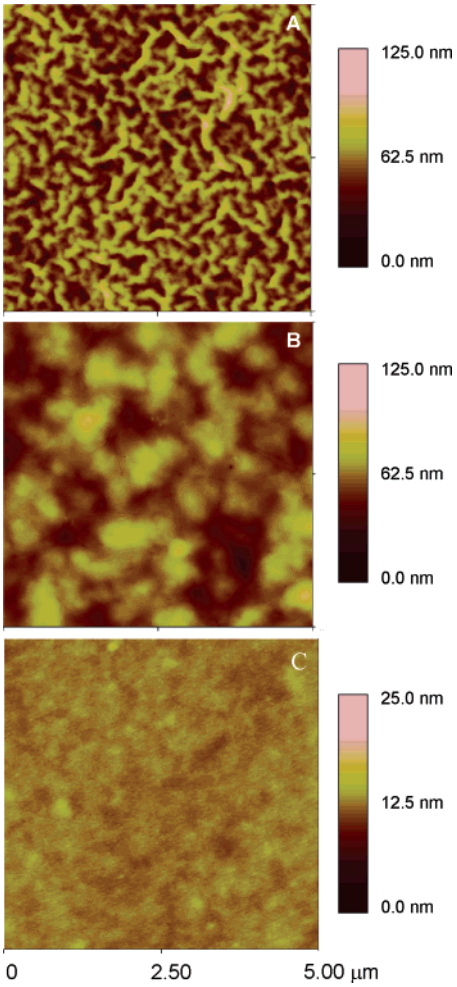

Figure 2. AFM images showing surface morphology of (A) system II, (B) system III, and (C) system IV. Films were built from polyelectrolyte buffered solutions at pH 7.2 and NaCl content 0.15 M. Thickness and rms roughness measurements of films are summarized in Table 2.

The annealing process in the multilayers is slow; neutron reflectivity studies show the diffusion constants, D, for polyelectrolytes in PSS/PDADMA systems fall between 2 × 10^{-17} and 6 × 10^{-17} cm^2 s^{-1} and they are salt-concentration-dependent.[38] In the PEI/polynucleotide systems, the polyelectrolytes are held together, in addition to electrostatic interactions, by H-bonding; therefore, one expects to obtain lower values for D, and hence the smoothing observed in particular for [PEI/poly(A)/poly(U)]$_7$ is due to the long period of annealing in the presence of NaCl inducing both interdiffusion and/or interpenetration of polymers and further H-bonding between base pairs of poly(A) and poly(U). In the case of [PEI/poly(AU)]$_{10}$, the rms roughness remains constant after annealing of the multilayer.

Conformational Changes. PEI is expected to distort the helical conformation of polynucleotides when interacting with them.[49] In order to investigate conformational changes, we

Table 2. Thickness and RMS Roughness Measurements Recorded before and after Annealing

	$[PEI/poly(A)/PEI/poly(U)]_5$	$[PEI/poly(AU)]_{10}$	$[PEI/poly(A)/poly(U)]_7$
thickness before annealing (nm)	203	193	260
thickness after annealing (nm)	172	127	115
roughness before annealing (nm)	12	5	30
roughness after annealing (nm)	8	4	7

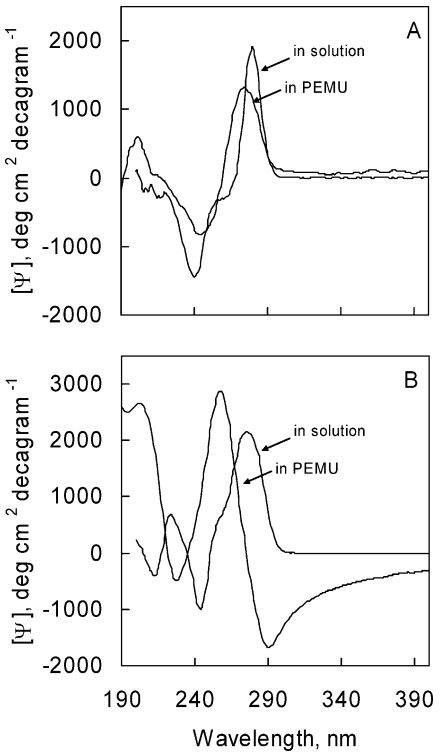

Figure 3. Specific ellipticity spectra of polynucleotides. (A) Spectra of poly(U) in solution and in a PEI multilayer matrix; (B) spectra of poly(AU) in solution and embedded in PEI multilayer. The spectra of solutions were from a mixture of 25 mM phosphate buffer solution at pH 7 containing 0.15 M NaCl.

collected circular dichroism (CD) spectra of both polyelectrolyte solutions and multilayers. The individual CD spectra of poly(A) and poly(U) in solution correspond to previously reported spectra of single-stranded helical poly(A) and poly(U) as well as the spectrum of the double-stranded poly(AU).[50] In Figure 3, we present the specific ellipticity for poly(U) and poly(AU) in solution and multilayers. Panel A depicts the spectra of poly(U) in solution and in a multilayer. A slight shift of wavelengths is present, which indicates changes in the stacking of the single-stranded helices with some retention of ordered conformation. In the case of poly(AU) (panel B), a complete change of spectrum is observed when it is deposited on PEI. Previously, PEI was shown to induce denaturation of double-stranded DNA at thymine (T) sites, which are chemically similar to uracil (U) sites (T has an additional methyl group attached to carbon C5 of the pyrimidine group).[49] We speculate that the PEI−poly(AU) interactions are inducing rupture of the double-stranded poly(AU) as a result of the PEI−nucleic base interactions, therefore inducing new conformational states.

Evidence for Specific Hydrogen Bonding. To further prove the presence of specific hydrogen bonding, we studied, in situ, the build-up of system III and the effect of hydrogen bonding by OWLS. In Figure 4, we show the growth of $[PEI/poly(A)/poly(U)]_2$. The data show the addition of a poly(A) layer onto the PEI followed by a slight increase in thickness when poly(U) is pumped through the cell, consistent with a thin adsorbed layer of poly(U) with no overcompensation.

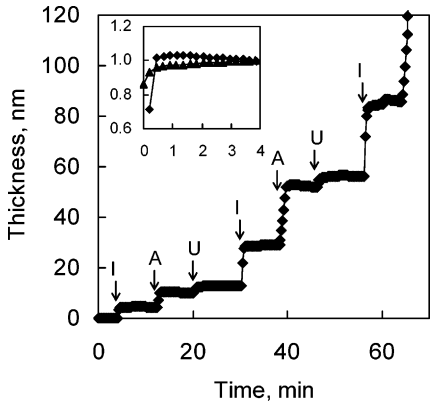

Figure 4. In situ build-up of [PEI/poly(A)/poly(U)]. Two complete layers are shown. The first step (I) corresponds to the deposition of PEI onto the negatively charged wafer surface; the second step (A), to the addition of poly(A); and the third step (U),to the addition of poly(U), from polyelectrolyte solutions at 0.15 M NaCl and 25 mM phosphate buffer at pH 7. Each deposition was followed by a 4-min rinse with 25 mM phosphate buffer at pH 7. Similar growth is observed when deposition order of poly(A) and poly(U) is reversed. (Inset) Relative additions of (◆) poly(A) and (▲) poly(U).

An interesting observation is the small amount of poly(U) added on poly(A); one expects to see a 1:1 poly(A):poly(U) ratio as one uridylic base can be bound to one adenylic base. Also, as we see in the inset of Figure 4, the deposition of poly(A) onto PEI is more or less an instantaneous addition compared to that of poly(U) on poly(A). Clearly, different factors are controlling the addition of poly(U) to the multilayer surface. Electrostatic repulsions between the negatively charged backbones of poly(A) and poly(U) might be a first factor, inhibiting poly(U) interdiffusion in poly(A) unlike poly(A) interdiffusion in PEI, and a second factor might be the thermodynamics and kinetics of base pairing.

In order to see whether the addition of poly(U) is electrostatic or due to specific H-bonding, we performed a second set of experiments by OWLS. In Figure 5, a first layer of PEI was followed by two additions of poly(A). No growth was observed when the second aliquot of poly(A) was pumped through the flow cell, indicating that the first flow of poly(A) was enough to neutralize the surface charges of PEI. When poly(U) was introduced, an increase in film thickness was observed. The increase can be associated only with nonelectrostatic interactions; hence, H-bonding is the driving force for the growth of this particular step.

To further prove the presence of specific hydrogen bonding between poly(A) and poly(U), poly(U) was substituted with poly(cytidylic acid), poly(C), and in situ experiments with poly(A) were conducted. Poly(C) is not complementary to poly(A); therefore, one does not expect to see a growth of the film when poly(C) is passed through the flow cell. Indeed, no growth was observed on a layer of poly(A) when poly(C) was pumped through, but when poly(U) was introduced, an increase was recorded (not shown).

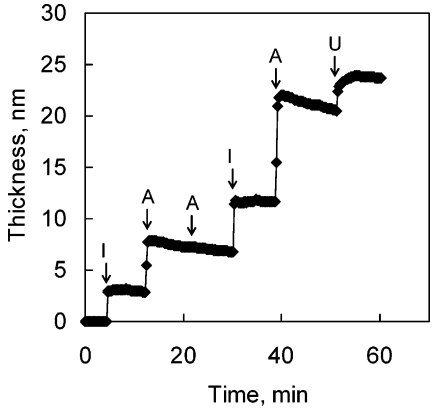

Figure 5. Spectrum of in situ build-up of system III: (I) addition of PEI onto the surface of the sensor chip; (A) adsorption of poly(A); (U) adsorption of poly(U). Each deposition was followed by a 4-min rinse with 25 mM phosphate buffer at pH 7.

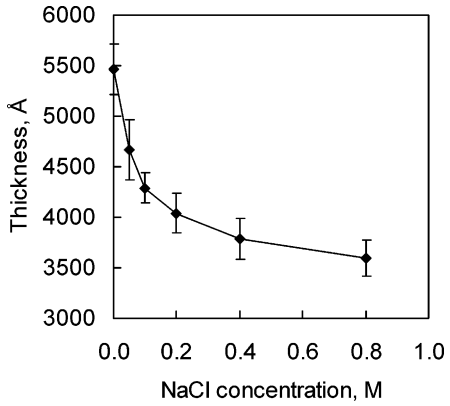

Figure 6. Thicknesses of $[PEI/poly(A)/poly(U)]_7$ built up at different NaCl concentrations in 25 mM phosphate buffer, pH 7.2, on Si substrates. The solid line is a guide to the eye.

The thermodynamics and kinetics of base pairing might limit the amount of poly(U) deposited on the surface of the film. Thorough studies have been conducted to understand the effect of nucleotide base concentration, temperature, and ionic strength on the structure of single strands (coil−helix transitions) and double-helix formation of oligonucleotides in solution.[51] It is well-known that at low ionic strength polynucleotides prefer to be single strands. As the salt concentration is increased, the thermodynamics of the system, explained as increased shielding of electrostatic repulsion, favors double-helix formation. In this study, we built multilayer films at different ionic strengths to investigate the effect of salt concentration on the build-up of the films (Figure 6).

The effect of salt concentration on polyelectrolyte multilayer growth is well investigated,[16,18] and further studies are being conducted to thoroughly understand kinetics of processes occurring within multilayers such as ion doping, water intake, and swelling phenomena. It is believed that the surface excess charge, responsible for the multilayer growth, increases as salt is added to the solution. Parallel to its presence on the surface, the excess charge is also extended into the bulk of the multilayer as the salt counterions enable interpenetration of polyelectrolytes.[17,22]

In our study, charge overcompensation is clearly present as $[PEI/poly(U)]_x$ and $[PEI/poly(A)/PEI/poly(U)]_x$ multilayers are assembled. But as we build-up PEMUs via [PEI/poly(A)/poly(U)] deposition sequence at different salt concentrations, we observe a decrease in the total film thickness. In previous studies, Kharlampieva and Sukhishvili[27,28] described the competition between nonspecific H-bonding and electrostatic interactions, where switching between H-bonding and electrostatics was achieved by altering the pH of the assembly environment. In these studies, no decrease in film thickness was reported. In another study, Izumrudov et al.[41] showed the variation of adsorbed amount of polyelectrolytes with increasing salt concentration. A maximum was observed for polymers of different molecular weights, followed by a decrease until complete dissolution of the complexes at 0.5 M NaCl.

The thickness of the PEI/poly(A)/poly(U) multilayers decreases and plateaus at high salt concentration. An explanation for the observed decrease is the presence of two competing factors, induced by the increase in salt concentration. Increase of salt concentration during build-up of PEMUs yields thicker films due to interpenetration; but as the amount of salt is increased in systems of polynucleotides, hydrogen bonding is favored. H-bonding interactions are stronger, so the ability to diffuse through the polymer network is decreased. Hence the degree of interpenetration is lower and thinner films are formed. At sufficiently high salt concentration, thickness ultimately reaches a plateau where the net effect of the two competing factors remains constant.

Conclusion

In this paper, we were able to build and investigate multilayers assembled from homopolynucleotides to study the specific hydrogen bonding between complementary nucleotides, adenylic and uridylic bases, embedded in a PEI matrix. In addition to morphological and conformational studies, we analyzed the interactions within the multilayers by circular dichroism and optical waveguide lightmode spectroscopy. Specific H-bonding within the multilayers was further analyzed, and the effect of ionic strength on the build-up of the PEI/poly(A)/poly(U) was studied. The experiments show a decrease of film thickness, contrary to the phenomenon observed for electrostatic-only systems such as PSS/PDADMA multilayers. With increasing salt concentration, H-bonding between the nucleotide bases is favored and polyelectrolyte interpenetration decreases, resulting in a decrease of film thickness which ultimately reaches a plateau at relatively high salt (NaCl) concentrations.

Acknowledgment. This work was supported by a grant from the National Science Foundation (DMR 0309441) and the Florida State University Program Enhancement grant.

References and Notes

(1) Schouten, S.; Stroeve, P.; Longo, M. L. *Langmuir* **1999**, *15*, 8133−8139.
(2) Demers, L. M.; Ginger, D. S.; Park, S. J.; Li, Z.; Chung, S. W.; Mirkin, C. A. *Science* **2002**, *296*, 1836−1838.
(3) Zhou, X.; Wu, L.; Zhou, J. *Langmuir* **2004**, *20*, 8877−8885.
(4) Boon, E. M.; Ceres, D. M.; Drummond, T. G.; Hill, M. G.; Barton, J. K. *Nat. Biotechnol.* **2000**, *18*, 1096−1100.
(5) Pedano, M. L.; Rivas, G. A. *Biosens. Bioelectron.* **2003**, *18*, 269−277.
(6) Pedano, M. L.; Rivas, G. A. *Sensors* **2005**, *5*, 424−447.
(7) Hartwich, G.; Caruana, D. J.; de Lumley-Woodyear, T.; Wu, Y.; Campbell, C. N.; Heller, A. *J. Am. Chem. Soc.* **1999**, *121*, 10803−10812.
(8) Langer, R. *Science* **2001**, *293*, 58−59.
(9) Jewell, C. M.; Zhang, J.; Fredin, N. J.; Lynn, D. M. *J. Controlled Release* **2005**, *106*, 214−223.
(10) Safinya, C. R. *Curr. Opin. Struct. Biol.* **2001**, *11*, 440−448.
(11) Garnett, M. *Int. J. Nanosci.* **2005**, *4*, 855−861.
(12) Lao, R.; Song, S.; Wu, H.; Wang, L.; Zhang, Z.; He, L.; Fan, C. *Anal. Chem.* **2005**, *77*, 6475−6480.

(13) Johnson, P. A.; Gaspar, M. A.; Levicky, R. *J. Am. Chem. Soc.* **2004**, *126*, 9910−9911.
(14) Vinogradova, O. I.; Lebedeva, O. V.; Vasilev, K.; Gong, H.; Garcia-Turiel, J.; Kim, B.-S. *Biomacromolecules* **2005**, *6*, 1495−1502.
(15) van den Beucken, J. J. J. P.; Vos, Matthijn, R. J.; Thune, P., C.; Hayakawa, T.; Fukushima, T.; Okahata, Y.; Walboomers, X. F.; Sommerdijk, N. A. J. M.; Nolte, Roeland, J. M.; Jansen, J. A. *Biomaterials* **2006**, *27*, 691−701.
(16) Decher, G. *Science* **1997**, *277*, 1232−1237.
(17) Decher, G., Schlenoff, J. B., Eds. *Multilayer Thin Films: Sequential Assembly of Nanocomposite Materials*; Wiley−VCH: Weinheim, Germany, 2003.
(18) Bertrand, P.; Jonas, A.; Laschewsky, A.; Legras, R. *Macromol. Rapid Commun.* **2000**, *21*, 319−348.
(19) Farhat, T. R.; Schlenoff, J. B. *Langmuir* **2001**, *17*, 1184−1192.
(20) Farhat, T.; Yassin, G.; Dubas, S. T.; Schlenoff, J. B. *Langmuir* **1999**, *15*, 6621−6623.
(21) Dubas, S. T.; Schlenoff, J. B. *Macromolecules* **1999**, *32*, 8153−8160.
(22) Schlenoff, J. B.; Dubas, S. T. *Macromolecules* **2001**, *34*, 592−598.
(23) Sui, Z.; Schlenoff, J. B. *Langmuir* **2004**, *20*, 6026−6031.
(24) Ostrander, J. W.; Mamedov, A. A.; Kotov, N. A. *J. Am. Chem. Soc.* **2001**, *123*, 1101−1110.
(25) Lojou, E.; Bianco, P. *Langmuir* **2004**, *20*, 748−755.
(26) Clark, S. L.; Hammond, P. T. *Langmuir* **2000**, *16*, 10206−10214.
(27) Kharlampieva, E.; Sukhishvili, S. A. *Langmuir* **2004**, *20*, 10712−10717.
(28) Kharlampieva, E.; Sukhishvili, S. A. *Macromolecules* **2003**, *36*, 9950−9956.
(29) Kozlovskaya, V.; Ok, S.; Sousa, A.; Libera, M.; Sukhishvili, S. A. *Macromolecules* **2003**, *36*, 8590−8592.
(30) Quinn, J. F.; Caruso, F. *Aust. J. Chem.* **2005**, *58*, 442−446.
(31) Stockton, W. B.; Rubner, M. F. *Macromolecules* **1997**, *30*, 2717−2725.
(32) Sukhishvili, S. A.; Granick, S. *Macromolecules* **2002**, *35*, 301−310.
(33) Wang, L. Y.; Wang, Z. Q.; Zhang, X.; Shen, J. C.; Chi, L.; Fuchs, H. *Macromol. Rapid Commun.* **1997**, *18*, 509−514.
(34) Fischer, P.; Laschewsky, A. *Macromolecules* **2000**, *33*, 1100−1102.
(35) Lowack, K.; Helm, C. A. *Macromolecules* **1998**, *31*, 823−833.
(36) Johnston, A. P. R.; Read, E. S.; Caruso, F. *Nano Lett.* **2005**, *5*, 953−956.
(37) Dubas, S. T.; Schlenoff, J. B. *Langmuir* **2001**, *17*, 7725−7727.
(38) Jomaa, H. W.; Schlenoff, J. B. *Macromolecules* **2005**, *38*, 8473−8480.
(39) Schlenoff, J. B.; Ly, H.; Li, M. *J. Am. Chem. Soc.* **1998**, *120*, 7626−7634.
(40) Lebedeva, O. V.; Kim, B.-S.; Vasilev, K.; Vinogradova, O. I. *J. Colloid Interface Sci.* **2005**, *284*, 455−462.
(41) Izumrudov, V.; Kharlampieva, E.; Sukhishvili, S. A. *Macromolecules* **2004**, *37*, 8400−8406.
(42) Cochin, D.; Laschewsky, A. *Macromol. Chem. Phys.* **1999**, *200*, 609−615.
(43) McAloney, R. A.; Sinyor, M.; Dudnik, V.; Goh, M. C. *Langmuir* **2001**, *17*, 6655−6663.
(44) Caruso, F.; Furlong, D. N.; Ariga, K.; Ichinose, I.; Kunitake, T. *Langmuir* **1998**, *14*, 4559−4565.
(45) Kim, D. K.; Han, S. W.; Kim, C. H.; Hong, J. D.; Kim, K. *Thin Solid Films* **1999**, *350*, 153−160.
(46) Kellogg, G. J.; Mayes, A. M.; Stockton, W. B.; Ferreira, M.; Rubner, M. F.; Satija, S. K. *Langmuir* **1996**, *12*, 5109−5113.
(47) Mills, J. B.; Vacano, E.; Hagerman, P. J. *J. Mol. Biol.* **1999**, *285*, 245−257.
(48) Abels, J. A.; Moreno-Herrero, F.; Van, der Heijden, T.; Dekker, C.; Dekker: N. H. *Biophys. J.* **2005**, *88*, 2737−2744.
(49) Prasad, T. K.; Gopal, V.; Rao, N. M. *FEBS Lett.* **2003**, *552*, 199−206.
(50) Berova, N., Nakanishi, K., Woody, R. W., Eds. *Circular Dichroism: Principles and Applications*, 2nd ed.; Wiley−VCH: New York, 2000.
(51) Bloomfield, V. A.; Crothers, D. M.; Tinoco, I., Jr. *Nucleic Acids: Structures, Properties, and Functions*; University Science Books: Sausalito, CA, 2000.

BM0604909